Electronic Supplementary Material (ESI) for Journal of Materials Chemistry A.

Supplementary Information

Low Cost, Facile, Environmentally Friendly All Biomass-based Squid Ink-Starch Hydrogel for Efficient Solar-Steam Generation

Yuanlu Xu, [#a] Xin Xiao,[#a] Xinfei Fan,*[,a] Yi Yang,[a] Chengwen Song,*[,a] Yaofang Fan,[b] Yanming Liu*[,b]

[a] College of Environmental Science and Engineering, Dalian Maritime University, Dalian 116026, China

[b] Key Laboratory of Industrial Ecology and Environmental Engineering (Ministry of Education, China), School of Environmental Science and Technology, Dalian University of Technology, Dalian 116024, China

*Corresponding author e-mail: fxf0909@dlmu.edu.cn, chengwensong@dlmu.edu.cn, liuyanm@dlut.edu.cn

[#]These authors contributed equally to this work.

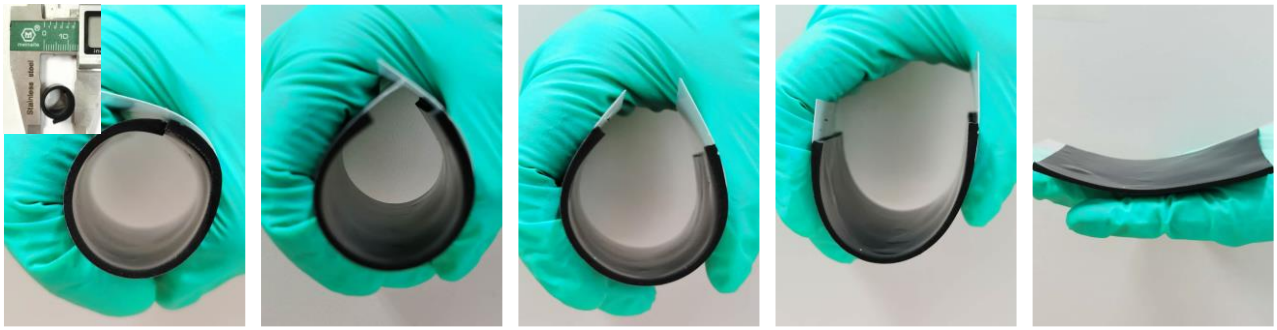

Figure S1. Images of the curving hydrogel.

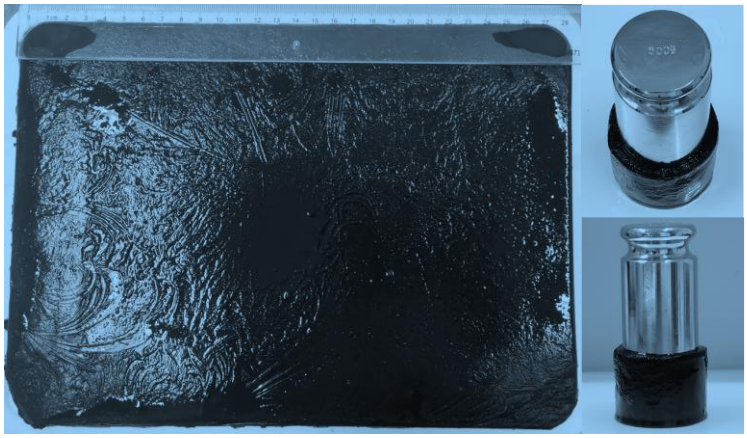

Figure S2. Photograph of large-sized composite hydrogel.

Figure S3. Photographs of hybrid hydrogels in various leaf forms.

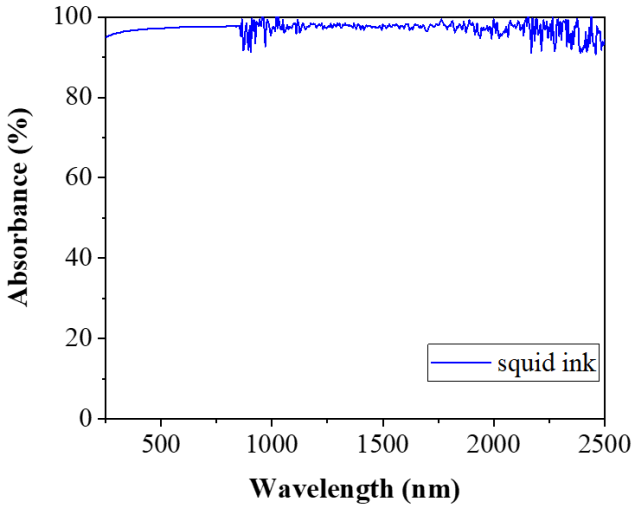

Figure S4. Light absorbance of squid ink.

Supplementary Note

Note 1. Effect of mass content of squid ink on evaporation performance.

Figure S5 displayed that the sample (1:10) presented more mass loss and quicker evaporation rate in the initial ~10 min irradiation compared to the sample (1:20). This was because the fresh samples were saturated with water, and the high squid ink/starch ratio means better light absorption for evaporation promotion. However, after ~10 min irradiation, the evaporation performance of sample (1:10) deteriorated with both parameters worse than those of sample (1:20). The plausible reason was insufficient water supply for evaporation. Moreover, Figure 1d, 1e, and S6 displayed increasing the squid ink/starch ratio resulted in an enlarged micron-pore sizes, which were 93.6 ± 17.6 μm, 97.5 ± 21.6 μm, 111.2 ± 20.1 μm, and 127.0 ± 15.1 μm for the ratio value of 0 (pure starch), 1:100, 1:20, and 1:10, respectively. For evaporation performance, although a large pore size negatively influences the capillary force for wicking water (Figure S9), the evaporation rate increased with squid ink/starch ratio until the ratio value to 1:20 (Figure 2e). This was because increasing squid ink in the hydrogel can significantly improve the light absorption, which played a more important role than wicking in the evaporation performance with the squid ink/starch ratio below 1:20. When the squid ink/starch ratio reached to 1:10, the evaporation rate was limited by the insufficient water transport rate due to the weakened wicking from its large micron-pore size, resulting in a declined evaporation rate.

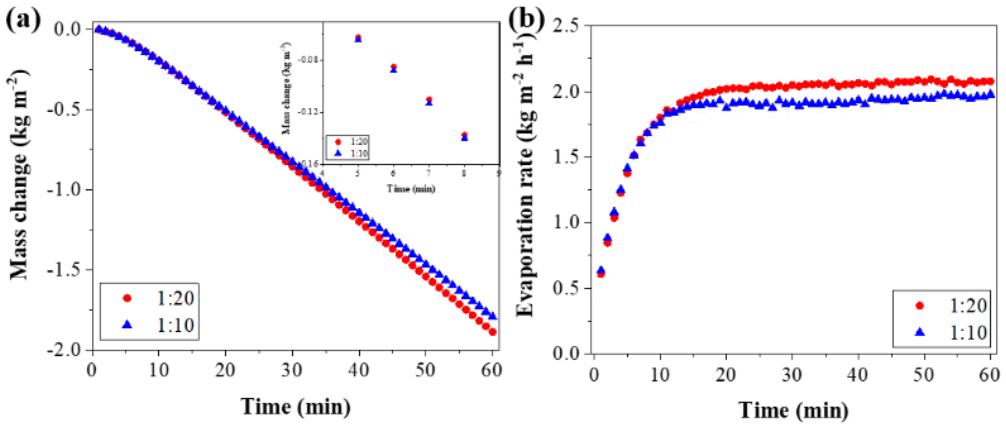

Figure S5. Comparison of mass loss (a) and evaporation rate (b) of hydrogels with squid ink to starch ratio of 1:20 and 1:10.

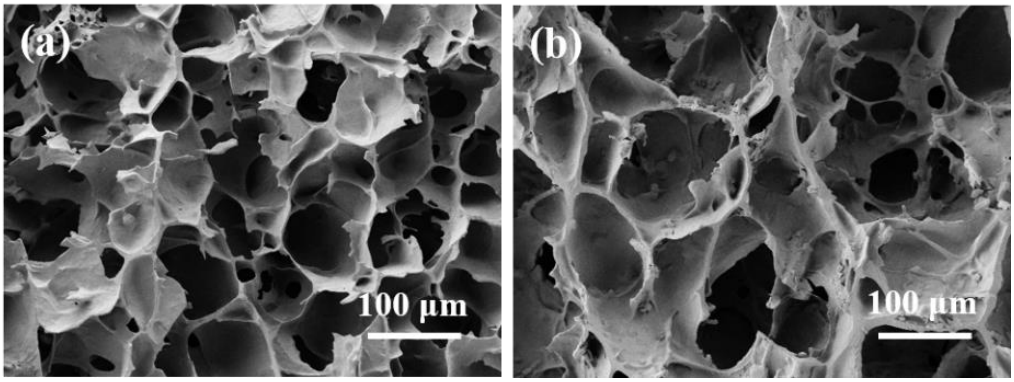

Figure S6. SEM images of hybrid hydrogel with different squid ink/starch ratio of 1:100 (a) and 1:10 (b).

Note S2. Thermal conductivity measurement.

According to the reported work,[1] the thermal conductivity of hydrogels was measured at room temperature of 25 °C using home-made test-apparatus as shown in Figure S7a. The sample (15 mm (Length) × 15 mm (width) × 10 mm (thickness)) was sandwiched between two squared-shape glass slabs (15 mm (Length) × 15 mm (width) × 1 mm (thickness)). The top side was coated with a black rubber by which can absorb light and convert into heat, while the bottom side contacted with an ice-water bath as cooling source. For wetted samples, their sidewalls were covered with thin plastic wrap to prevent water evaporation. Since the system reached to thermal equilibrium in 1 h, IR images (Figure S7b) was taken for analyzing thermal conductivity by Fourier equation:

$$q = -k_1 \times (\mathrm{d}T/\mathrm{d}x) = -k_1 \times (T_2-T_1)/t_1$$

where k_1 is the thermal conductivity of glass (1.0 W m^{-1} k^{-1}), T_1 and T_2 denote the average temperature at the interfaces s_1 and s_2, and t_1 is the thickness of glass (1.0 mm).

The thermal conductivity of the samples was calculated by:

$$k = -q \times (\mathrm{d}x/\mathrm{d}T) = -q \times (t_2/(T_3-T_2))$$

where T_3 is the average temperature at the interface s_3, and t_2 is the thickness of samples (10 mm).

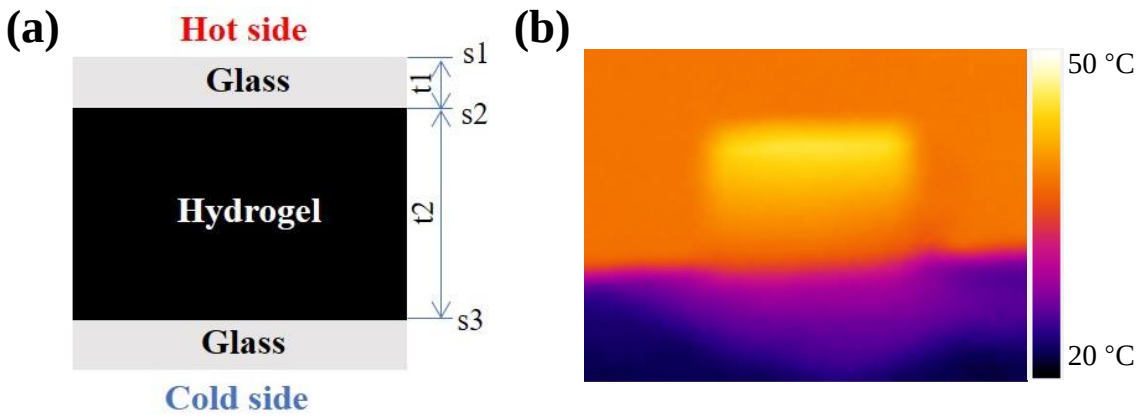

Figure S7. Schematic diagram of home-made test-apparatus for thermal conductive measurement (a), and IR image of the wetted sample at thermal equilibrium state.

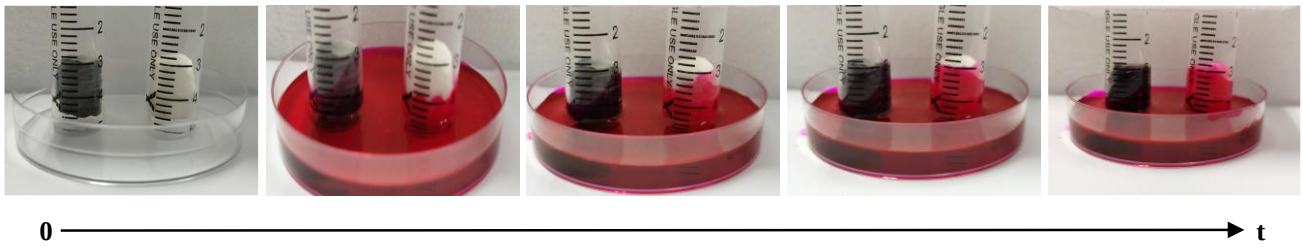

Figure S8. Water wicking test of the hydrogels

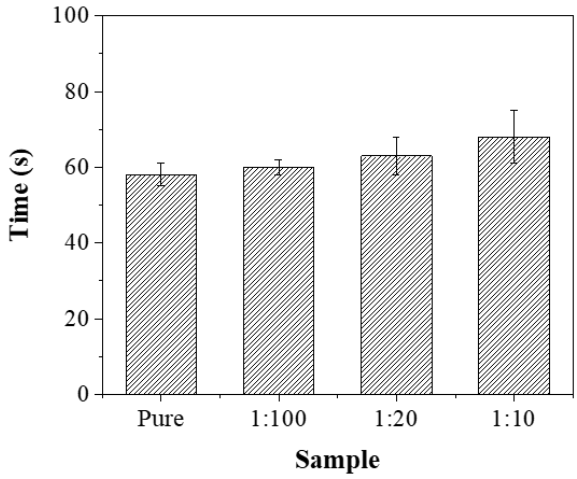

Figure S9. Wetting time for hydrogels with different squid ink/starch ratio during wicking test.

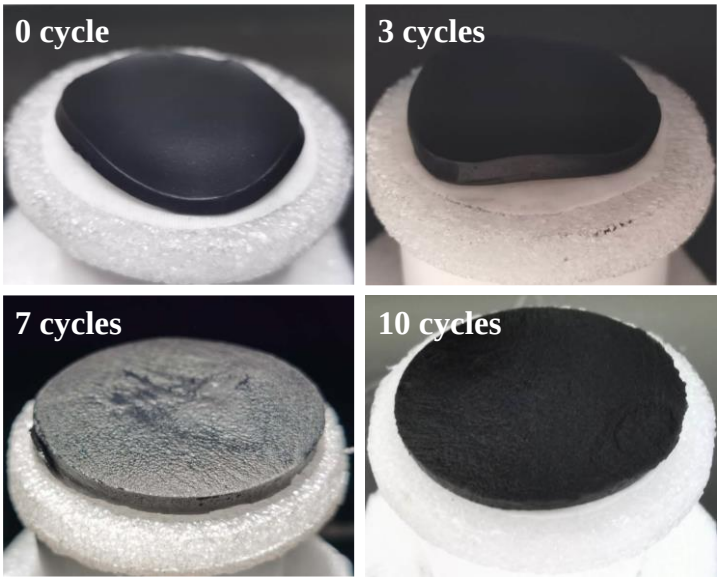

Figure S10. Photographs of evaporators by different freeze-thaw cycles after 60 min under 1.0 sun irradiation.

Note S3. Estimation of equivalent evaporation enthalpy.

The equivalent evaporation enthalpy was estimated as described in the reported works.[2, 3] The bulk water and wetted hydrogels with same superficial area were simultaneously putted into a temperature humidity chamber with temperature of ca. 25 °C and humidity of ca. 45%. The equivalent evaporation enthalpy (ΔH_{equ}) was calculated by the following equation:

$$U_{in} = \Delta H_{water} \times m_0 = \Delta H_{equ} \times m_{hydrogel}$$

where U_{in} is the identical power input, ΔH_{water} and ΔH_{equ} are the respective evaporation enthalpy for bulk water and hydrogels, m_0 and $m_{hydrogel}$ are the mass loss for bulk water and hydrogels, respectively.

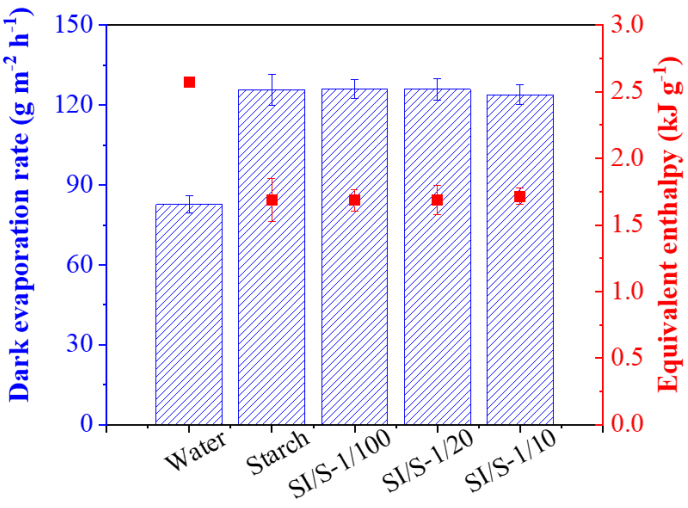

Figure S11. Dark water evaporation rate and the calculated equivalent enthalpy of the water evaporation in hydrogel evaporators.

Note S4. Analysis of heat loss.

To reflect the evaporation performance in two-dimensional form, the evaporation test was performed by wrapping the sidewall of the evaporator with plastic film to reduce steam generation from side surface, during which the evaporation rate and corresponding energy efficiency were 1.81 kg m^{-2} h^{-1} and 83.7%, respectively. Meanwhile, the energy loss of the evaporation system under light irradiation mainly includes radiation loss (P_{rad}), convection loss (P_{conv}) and conduction loss (P_{cond}), detailed energy loss analysis was performed as following calculations.

1) Radiation

The radiation flux (P_{rad}) was calculated by Stefan-Boltzmann law.

$$P_{rad} = \varepsilon\sigma(T_1^4 - T_2^4)$$

where P_{rad} represents the radiation heat flux, ε denotes the emissive rate (0.95 in this work), σ is the Stefan-Boltzmann constant (assumed to be 5.67×10^{-8} W m^{-2} K^{-4}), T_1 and T_2 are the average temperature of the absorber (~319.1 K) and the ambient temperature near the light absorber/air interface (~311.4 K), respectively. Based on this equation, the radiation heat flux was estimated to be ~52 W m^{-2}, and the radiation loss rate was about 5.2%.

2) Convection

The convection loss (P_{conv}) was obtained according to the Newton's law of cooling.

$$P_{conv} = h(T_1 - T_2)$$

where P_{conv} denotes convection heat flux, h represents the convection heat transfer coefficient (assumed to be 10 W m^{-2} K^{-1}). Accordingly, the estimated convection heat was about 77 W m^{-2}, and the convection loss rate was ~7.7%.

3) Conduction

Conduction loss (P_{cond}) was based on Fourier's law.

$$P_{cond} = Cm\Delta T$$

where C denotes the specific heat capacity of water (4.2 J ℃$^{-1}$ g^{-1}), m is the weight of bulk water, and ΔT represents the temperature change of bulk water after stable steam generation. In this work, temperature change of bulk water body was negligible due to a PS foam blocking the downward conduction loss. Thus, the conduction loss rate herein was considered as 0.

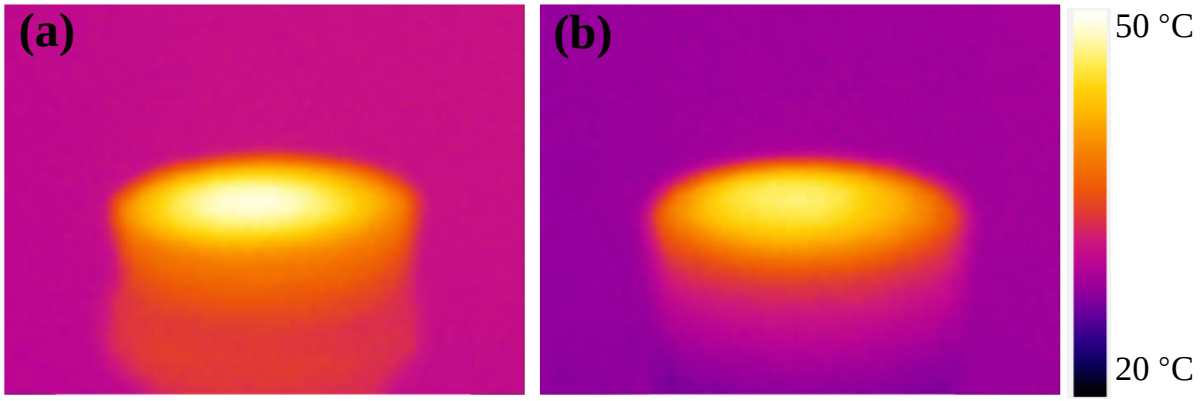

Figure S12. IR images of top surface of middle (a) and high (b) hybrid evaporators under 1.0 sun illumination after 60 min.

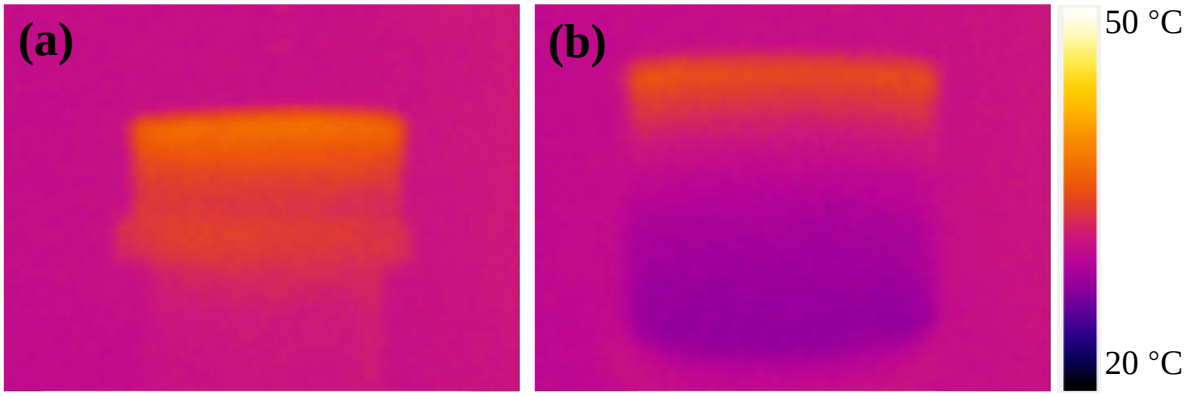

Figure S13. IR images of sidewall of middle (a) and high (b) hybrid evaporators under 1.0 sun illumination after 60 min.

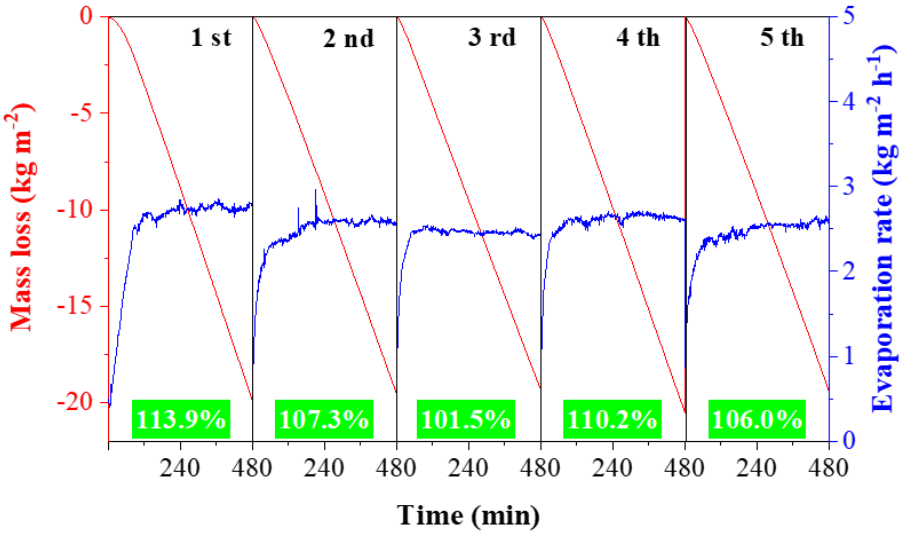

Figure S14. Evaporation-induced mass changes, evaporation rate and energy efficiency of high squid ink/starch hydrogel evaporator under 1.0 sun irradiation.

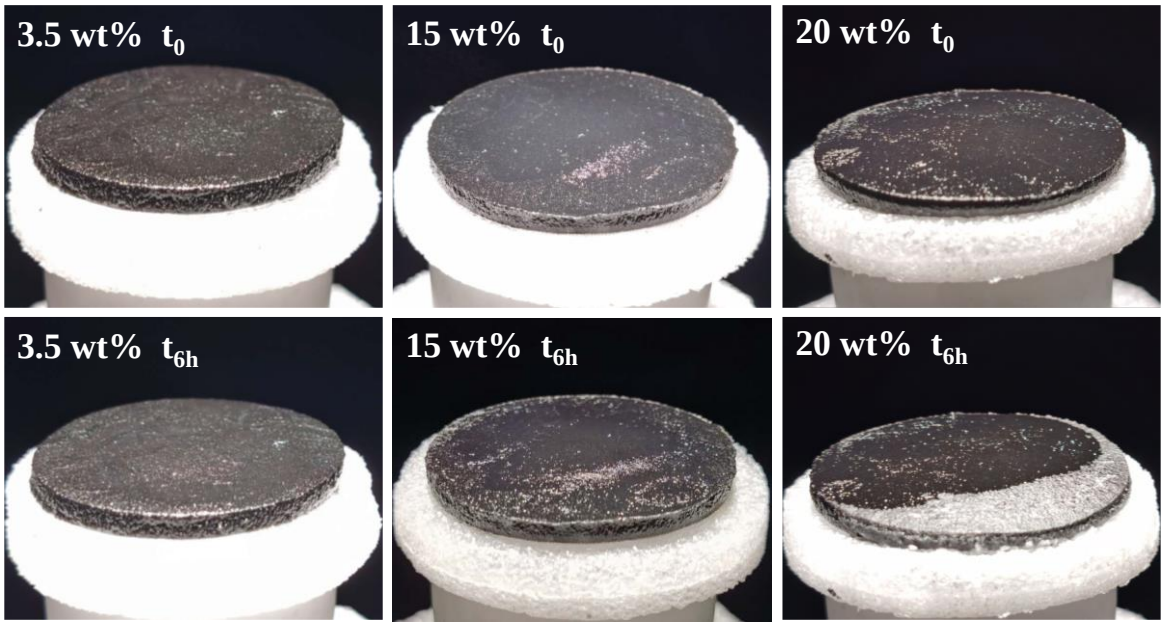

Figure S15. Photographs of the evaporative surface of the evaporator in different salinity conditions with 1.0 sun irradiation for 6 h.

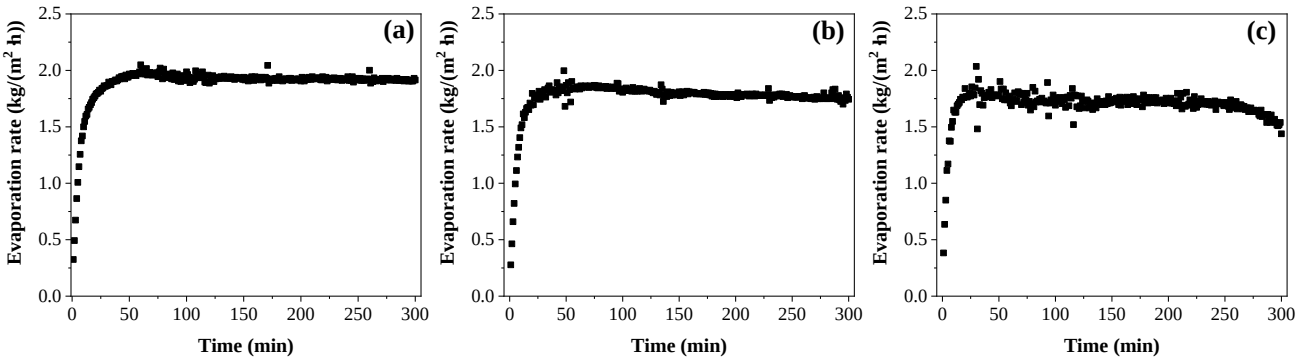

Figure S16. Evaporation rates of hydrogel evaporator for different salinity: 3.5 wt% (a), 15.0 wt% (b), and 20.0 wt% (c).

Figure S17. Self-cleaning test of composite hydrogel.

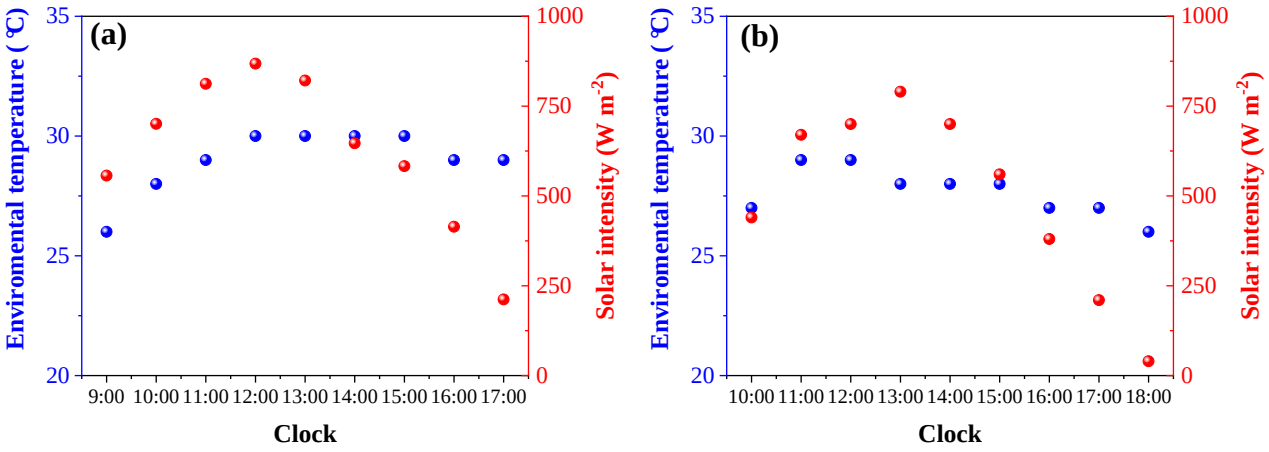

Figure S18. Changes in environmental temperature and solar intensity on the roof of School Environmental Science and Engineering at Dalian Marine University: (a) sun day (4 Aug. 2020) and (b) cloud day (30 Jul. 2020).

References

1. Xu Ying, Tang Chuyang, Ma Jiaxiang, Liu Dongqing, Qi Dianpeng, You Shijie, Cui Fuyi, Wei Yen, Wang Wei, Low-Tortuosity Water Microchannels Boosting Energy Utilization for High Water Flux Solar Distillation. *Environmental Science & Technology* **2020,** *54*, 5150-5158.
2. Zhao Fei, Zhou Xingyi, Shi Ye, Qian Xin, Alexander Megan, Zhao Xinpeng, Mendez Samantha, Yang Ronggui, Qu Liangti, Yu Guihua, Highly efficient solar vapour generation via hierarchically nanostructured gels. *Nature Nanotechnology* **2018,** *13*, 489-495.
3. Guo Youhong, Zhou Xingyi, Zhao Fei, Bae Jiwoong, Rosenberger Brian, Yu Guihua, Synergistic Energy Nanoconfinement and Water Activation in Hydrogels for Efficient Solar Water Desalination. *ACS Nano* **2019,** *13*, 7913-7919.